Contextual and Variational Contrast Enhancement

Turgay Celik and Tardi Tjahjadi *Senior Member, IEEE*

Abstract

This paper proposes an algorithm which enhances the contrast of an input image using inter-pixel contextual information. The algorithm uses a two-dimensional (2D) histogram of the input image constructed using mutual relationship between each pixel and its neighbouring pixels. A smooth 2D target histogram is obtained by minimizing the sum of Frobenius norms of the differences from the input histogram, and the uniformly distributed histogram. The enhancement is achieved by mapping the diagonal elements of the input histogram to the diagonal elements of the target histogram. Experimental results show that the algorithm produces better or comparable enhanced images than four state-of-the-art algorithms.

Index Terms

Contrast enhancement, histogram equalization, image quality enhancement, face recognition.

I. Introduction

Contrast enhancement is used to either increase the contrast of an image with low dynamic range or to bring out image details that would otherwise be hidden [1]. The enhanced image looks subjectively better than the original image as the grey level differences (i.e., the contrast) among objects and background are increased.

The conventional approach to enhance the contrast in an image is to manipulate the grey-level of individual pixels. Global histogram equalization (GHE) [1] uses an input-to-output mapping derived from the cumulative distribution function (CDF) of the image histogram. Although GHE utilizes the available grey scale of the image, it tends to over-enhance the image if there are large peaks in the histogram, resulting in a harsh and noisy appearance of the enhanced image. It does not always produce satisfactory enhancement for images with large spatial variation in contrast. Local histogram equalization (LHE) algorithms have been developed, e.g., [2], [3], to address the aforementioned problems. These algorithms use a small window that slides over every image pixel sequentially and the histogram of pixels within the current position of the window is equalized. LHE sometimes over-enhances some portion of the image and any noise, and may produce undesirable checkerboard effects.

Other algorithms that focus on improving GHE [4]–[9] can achieve satisfactory contrast enhancement, but the variation in the grey-level distribution may result in image degradation [10]. Dynamic histogram specification (DHS) [10] uses the desired histogram, generated dynamically from the input image, to modify the input image histogram. In order to retain the features in the input image histogram, DHS extracts the differential information from the input image histogram and incorporates additional parameters to control the enhancement such as the image original and the resultant gain control values. However, the degree of enhancement that can be achieved is not significant. In order to address the artefacts due to over-enhancement and saturation of grey levels of GHE, the original image histogram is modified by weighting and thresholding before the histogram equalization in [9]. The weighting and thresholding are performed by clamping the original image histogram at an

This work was supported by Warwick University Vice Chancellor Scholarship.

Turgay Celik and Tardi Tjahjadi are with the School of Engineering, University of Warwick, Coventry, CV4 7AL, United Kingdom. e-mail: Turgay Celik (celikturgay@gmail.com), Tardi Tjahjadi (t.tjahjadi@warwick.ac.uk).

upper threshold and at a lower threshold, and transforming all the values between these thresholds using a normalized power law function with an index. We refer the algorithm as weighted thresholded histogram equalization (WTHE). WTHE provides satisfactory enhancement with the carefully selected default parameter setting.

One group of algorithms decompose an input image into different subbands so as to modify, globally or locally, the magnitude of the desired frequency components of the image data using multiscale analysis [11]–[14]. These algorithms enable the simultaneous global and local contrast enhancement by transforming the appropriate subbands and in the appropriate scales. For example, the centre-surround Retinex algorithm [11] achieves lightness and colour constancy in images. However, the enhanced image may include "halo" artefacts, especially along boundaries between large uniform regions. A "greying out" can also occur resulting in the image of the scene tending to middle grey.

Optimisation methods have also been used for contrast enhancement. Convex optimisation is used in flattest histogram specification with accurate brightness preservation (FHSABP) [15] to transform the input image histogram into the flattest histogram, subject to a mean brightness constraint. This is followed by applying an exact histogram specification algorithm to preserve the image brightness. FHSABP behaves very similar to GHE when the grey levels of the input image are equally distributed. Since it is designed to preserve the average brightness, FHSABP may produce low contrast results when the average brightness is either too low or too high. Contrast enhancement in histogram modification framework (HMF) [16] minimizes a cost function to compute a target histogram. The cost function is composed of penalty terms of minimum histogram deviation from the original and uniform histograms, and histogram smoothness. Furthermore, the edge information is embedded into the cost function to weight pixels around region boundaries to address noise and black/white stretching [16]. In order to design a parameter free contrast enhancement algorithm, genetic algorithm (GA) is employed in [17] to find a target histogram which maximizes a contrast measure based on edge information. We refer this algorithm as contrast enhancement based on GA (CEBGA). CEBGA suffers from the drawbacks of GA based algorithms, namely dependency on initialization and convergence to a local optimum. Furthermore, the convergence time is proportional to the number of distinct grey levels in the input image.

All the above approaches use a 1-dimensional (1D) histogram. Other than HMF [16], they do not take into account the contextual information content in the image. HMF [16] uses the image edge information to weight the 1D histogram.

We propose a contextual and variational contrast enhancement algorithm (CVC) to improve the visual quality of input images as follows. Images with low-contrast are improved in terms of an increase in dynamic range. Images with sufficiently high contrast are also improved but not as much. The colour quality are improved in terms of colour consistency, higher contrast between foreground and background objects, larger dynamic range and more image details are visible. The enhancement process is based on the observation that contrast can be improved by increasing the grey-level differences between the pixels of an input image and their neighbours. Furthermore, for the purpose of image equalization, grey-level differences should be equally distributed over the entire input image. To realise these observations, a 2D histogram of the input image is constructed and modified with a priori probability which assigns higher probability to the high grey-level differences, and vice versa. In 2D histogram, for each grey-level in the input image, the distribution of other grey-levels in the neighbourhood of the corresponding pixel is computed. A smooth 2D target histogram is obtained by minimizing the sum of Frobenius norms of the differences from the 2D input histogram, and the 2D uniformly distributed histogram. The contrast enhancement is achieved by mapping the diagonal elements of the 2D input histogram to the diagonal elements of the 2D target histogram.

The paper is organized as follows. Section II presents the proposed CVC. Section III presents the subjective and quantitative comparisons of CVC with four state-of-the-art enhancement techniques. Section IV concludes the paper.

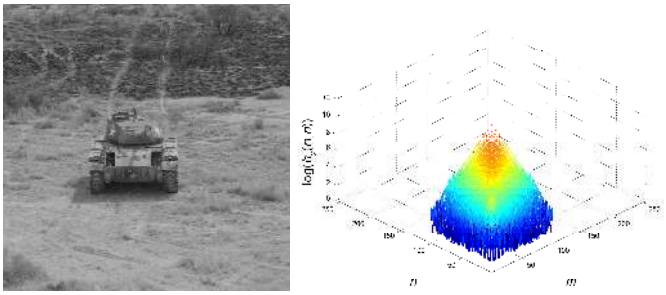

(a) (b)

Fig. 1. The input image (a) and its 2D histogram (b) using 7×7 neighbourhood. For display purpose, $h_{\mathrm{x}}(m,n)$ is shown in logarithmic scale.

II. Proposed Algorithm (CVC)

A. Grey-Scale Image Enhancement

Consider an input image, $\mathbf{X} = \{x(i,j) \mid 1 \leq i \leq H, 1 \leq j \leq W\}$, of size $H \times W$ pixels, where $x(i,j) \in [0, \mathbb{Z}^+]$ and assume that $\mathbf{X}$ has a dynamic range of $[x_d, x_u]$ where $x(i,j) \in [x_d, x_u]$. The objective of CVC is to generate an enhanced image, $\mathbf{Y} = \{y(i,j) \mid 1 \leq i \leq H, 1 \leq j \leq W\}$, which has a better visual quality than $\mathbf{X}$. The dynamic range of $\mathbf{Y}$ can be stretched or compressed into the interval $[y_d, y_u]$, where $y(i,j) \in [y_d, y_u]$, $y_d < y_u$ and $\{y_d, y_u\} \in [0, \mathbb{Z}^+]$. In this work, the enhanced image utilizes the entire dynamic range, e.g., for an 8-bit image $y_d = 0$, and $y_u = 2^8 - 1 = 255$.

Let $\mathcal{X} = \{x_1, x_2, \ldots, x_K\}$ be the sorted set of all possible K grey-levels that can occur in an input image $\mathbf{X}$ where $x_1 < x_2 < \ldots < x_K$, where $K = 256$ for an 8-bit image. The 2D histogram of the input image $\mathbf{X}$ is computed as

$$\mathbf{H}_{\mathrm{x}} = \left\{ h_{\mathrm{x}}(m,n) \mid 1 \leq m \leq K, 1 \leq n \leq K \right\}, \tag{1}$$

where $h_{\mathrm{x}}(m,n) \in [0, \mathbb{Z}^+]$ is the number of occurrences of the n^{th} grey-level (x_n) in the neighbourhood of the m^{th} grey-level (x_m). Different types of neighbourhood can be employed, however for a typical implementation of CVC $w \times w$ neighbourhood around each pixel is considered. For example, Fig. 1 shows the input image and its 2D histogram using 7×7 neighbourhood. The image has more bright regions than dark regions, thus its histogram has larger values located at higher grey-values. In homogeneous regions, the neighbours of each pixel have very similar grey-levels which result in higher peaks at diagonal or near-diagonal elements of the histogram.

For an improved contrast there should be larger grey-level differences between the pixel under consideration and its neighbours. Thus, the 2D histogram is modified according to

$$h_{\mathrm{x}}(m,n) = h_{\mathrm{x}}(m,n)\, h_{\mathrm{p}}(x_m, x_n) \tag{2}$$

and

$$h_{\mathrm{p}}(x_m, x_n) = (|x_m - x_n| + 1) / (x_K - x_1 + 1), \tag{3}$$

where $h_{\mathrm{p}}(x_m, x_n) \in [0,1]$ assigns a weight to the occurrences of (x_m, x_n) which is proportional to the modulus of the grey-level difference between x_m and x_n. The 2D histogram shown in Fig. 1(b) is updated as shown in Fig. 2(b) using the $h_{\mathrm{p}}(x_m, x_n)$ shown in Fig. 2(a). It is clear from Fig. 2(a) that $h_{\mathrm{p}}(x_m, x_n)$ assigns higher weights to the components according to their distance from the diagonal elements. Thus, $h_{\mathrm{p}}(x_m, x_n)$ enhances larger differences which results in greater contrast in the overall image.

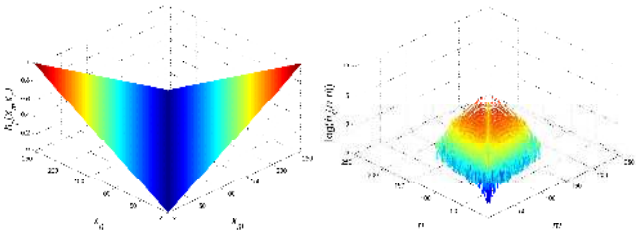

(a) (b)

Fig. 2. Updating the 2D histogram shown in Fig. 1(b): (a) $h_{\mathrm{p}}(x_m, x_n)$ computed using Eq. (3); and (b) Updated 2D histogram $h_{\mathrm{x}}(m,n)$ using Eq. (2). For display purpose, $h_{\mathrm{x}}(m,n)$ is shown in logarithmic scale.

The updated 2D histogram $\mathbf{H}_{\mathrm{x}}$ is normalized according to

$$h_{\mathrm{x}}(m,n) = h_{\mathrm{x}}(m,n) \Big/ \sum_{i=1}^{K}\sum_{j=1}^{K} h_{\mathrm{x}}(i,j) \tag{4}$$

to give a CDF

$$\mathcal{P}_{\mathrm{x}} = \left\{ P_{\mathrm{x}}(m) = \sum_{i=1}^{m}\sum_{j=1}^{m} h_{\mathrm{x}}(i,j) \;\middle|\; m = 1,\ldots,K \right\}. \tag{5}$$

Let $\mathcal{Y} = \{y_1, y_2, \ldots, y_K\}$ be the sorted set of all possible K grey-levels that can occur in output image $\mathbf{Y}$ where $y_1 < y_2 < \ldots < y_K$. In order to map the elements of $\mathcal{X}$ to the elements of $\mathcal{Y}$, it is necessary to determine a $K \times K$ target histogram $\mathbf{H}_{\mathrm{t}}$ and its CDF $\mathcal{P}_{\mathrm{t}}$. In order to equally enhance every possible occurrence of grey-levels of the input image pixels and their neighbours, $\mathbf{H}_{\mathrm{t}}$ can be selected as a 2D uniformly distributed histogram

$$\mathbf{H}_{\mathrm{u}} = \left\{ h_{\mathrm{u}}(m',n') = \frac{1}{K^2} \middle| 1 \le m' \le K, 1 \le n' \le K \right\}. \tag{6}$$

However, such a selection does not consider the contribution of the 2D input histogram. Instead, $\mathbf{H}_{\mathrm{t}}$ should have a minimum distance from the input histogram, i.e.,

$$\mathbf{H}_{\mathrm{t}} = \underset{\mathbf{H}}{\operatorname{argmin}} \|\mathbf{H} - \mathbf{H}_{\mathrm{x}}\|, \tag{7}$$

where $\|\cdot\|$ computes the norm. Motivated by the maximum entropy principle, $\mathbf{H}_{\mathrm{t}}$ should also have a minimum distance from the uniformly distributed histogram, i.e.,

$$\mathbf{H}_{\mathrm{t}} = \underset{\mathbf{H}}{\operatorname{argmin}} \|\mathbf{H} - \mathbf{H}_{\mathrm{u}}\|. \tag{8}$$

Furthermore, in order to satisfy a smooth mapping, $\mathbf{H}_{\mathrm{t}}$ should have minimum deviations between its components, i.e.,

$$\mathbf{H}_{\mathrm{t}} = \underset{\mathbf{H}}{\operatorname{argmin}} \|\mathbf{H}\mathbf{D}\|, \tag{9}$$

where $\mathbf{D} \in \mathbb{R}^{K \times K}$ is a $K \times K$ bidiagonal difference matrix

$$\mathbf{D} = \begin{bmatrix} d & -d & 0 & \cdots & 0 & 0 & 0 \\ 0 & d & -d & \cdots & 0 & 0 & 0 \\ \vdots & \vdots & \vdots & & \vdots & \vdots & \vdots \\ 0 & 0 & 0 & \cdots & 0 & d & -d \\ 0 & 0 & 0 & \cdots & 0 & 0 & d \end{bmatrix}, \tag{10}$$

where d is a constant which is set to 1. The matrix multiplication in Eq. (9) results in a matrix which holds differences between the horizontal elements of the matrix $\mathbf{H}$. The vertical elements can also be considered, however the enhancement result will not change significantly.

In order to determine the target histogram $\mathbf{H}_{\mathrm{t}}$, all the conditions are combined into the following optimization function

$$f\left(\mathbf{H}\right)=\alpha\left\|\mathbf{H}-\mathbf{H}_{\mathrm{x}}\right\|+\beta\left\|\mathbf{H}-\mathbf{H}_{\mathrm{u}}\right\|+\gamma\left\|\mathbf{D}\mathbf{H}\right\|, \tag{11}$$

where α, β and γ are weighting factors for the contributions from different conditions, and $\{\alpha,\beta,\gamma\}\in(0,1]$. The target histogram is obtained by minimizing $f\left(\mathbf{H}\right)$ according to

$$\mathbf{H}_{\mathrm{t}}=\underset{\mathbf{H}}{\mathrm{argmin}}f\left(\mathbf{H}\right). \tag{12}$$

The closed form solution to minimizing Eq. (12) is obtained by replacing the norm operation with square of the Frobenius norm (also known as Euclidean norm) which is defined as the square root of the sum of the absolute squares of its elements. Hence, the minimization of $f\left(\mathbf{H}\right)$ with respect to $\mathbf{H}$ is

$$f\left(\mathbf{H}\right)=\alpha\left\|\mathbf{H}-\mathbf{H}_{\mathrm{x}}\right\|_F^2+\beta\left\|\mathbf{H}-\mathbf{H}_{\mathrm{u}}\right\|_F^2+\gamma\left\|\mathbf{D}\mathbf{H}\right\|_F^2$$

or equivalently

$$\begin{aligned} f\left(\mathbf{H}\right) \;=\; & \alpha\ \mathrm{tr}\left(\left(\mathbf{H}-\mathbf{H}_{\mathrm{x}}\right)\left(\mathbf{H}-\mathbf{H}_{\mathrm{x}}\right)^{\mathrm{T}}\right)+\\ & \beta\ \mathrm{tr}\left(\left(\mathbf{H}-\mathbf{H}_{\mathrm{u}}\right)\left(\mathbf{H}-\mathbf{H}_{\mathrm{u}}\right)^{\mathrm{T}}\right)+\\ & \gamma\ \mathrm{tr}\left(\mathbf{H}\mathbf{D}\left(\mathbf{H}\mathbf{D}\right)^{\mathrm{T}}\right), \end{aligned} \tag{13}$$

where $\mathrm{tr}\left(\mathbf{A}\right)$ is trace of the matrix $\mathbf{A}$ and T is the transpose operator. The target histogram $\mathbf{H}_{\mathrm{t}}$ is obtained by solving

$$\nabla_{\mathbf{H}}f\left(\mathbf{H}\right)=\mathbf{0}, \tag{14}$$

where $\nabla_{\mathbf{H}}$ is the $K\times K$ Jacobian matrix, and $\mathbf{0}$ is the $K\times K$ zero matrix. Using the properties of matrix trace, the target histogram is derived from Eq. (14) (see the appendix for the detailed derivation) as

$$\begin{aligned} \mathbf{H}_{\mathrm{t}} \;&=\; \left(\left(\alpha+\beta\right)\mathbf{I}+\gamma\mathbf{D}\mathbf{D}^{\mathrm{T}}\right)^{-1}\left(\alpha\mathbf{H}_{\mathrm{x}}+\beta\mathbf{H}_{\mathrm{u}}\right)\\ &=\; \mathbf{R}^{-1}\left(\alpha\mathbf{H}_{\mathrm{x}}+\beta\mathbf{H}_{\mathrm{u}}\right)=\mathbf{S}\left(\alpha\mathbf{H}_{\mathrm{x}}+\beta\mathbf{H}_{\mathrm{u}}\right), \end{aligned} \tag{15}$$

where $\mathbf{R}$ is a $K\times K$ tridiagonal matrix in the form of

$$\mathbf{R}=\left(-d^2\gamma\right)\begin{bmatrix} r_0 & 1 & 0 & \cdots & 0 & 0 & 0\\ 1 & r_0 & 1 & \cdots & 0 & 0 & 0\\ \vdots & \vdots & \vdots & & \vdots & \vdots & \vdots\\ 0 & 0 & 0 & \cdots & 1 & r_0 & 1\\ 0 & 0 & 0 & \cdots & 0 & 1 & 1+r_0 \end{bmatrix}, \tag{16}$$

where $r_0=\left(2\gamma d^2+\alpha+\beta\right)/\left(-d^2\gamma\right)$. The inverse of a generalized tridiagonal matrix can be computed recursively [18]. Since $\mathbf{R}$ is a special case of the generalized tridiagonal matrix, letting $\mathbf{R}^{-1}=\mathbf{S}=\left\{s\left(m,n\right)\ \middle|\ 1\le m\le K,1\le n\le K\right\}$ gives $s\left(m,n\right)$ of the inverse matrix $\mathbf{S}$ as follows

$$s\left(m,n\right)=\begin{cases} \frac{(-1)^{m+n}}{(-d^2\gamma)}\frac{\theta(m-1)\phi(n+1)}{\theta(K)}, & m<n\\ \frac{1}{(-d^2\gamma)}\frac{\theta(m-1)\phi(m+1)}{\theta(K)}, & m=n\\ \frac{(-1)^{m+n}}{(-d^2\gamma)}\frac{\theta(n-1)\phi(m+1)}{\theta(K)}, & m>n, \end{cases} \tag{17}$$

where for $k=1\ldots K$

$$\theta\left(k\right)=\begin{cases} r_0\theta\left(k-1\right)-\theta\left(k-2\right), & k<K\\ \left(1+r_0\right)\theta\left(k-1\right)-\theta\left(k-2\right), & k=K, \end{cases} \tag{18}$$

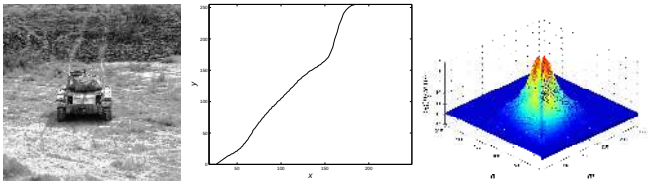

Fig. 3. Enhancing the input image in Fig. 1 (a) using CVC with $\alpha = \beta = \gamma = 1/3$: (a) Enhanced output image; (b) Input ($\mathcal{X}$) to output ($\mathcal{Y}$) grey-level data mapping; and (c) The 2D target histogram $\mathbf{H}_{\mathrm{t}}$.

and for $k = K \ldots 1$

$$\phi(k) = \begin{cases} (1 + r_0)\,\phi(k+1) - \phi(k+2), & k = K \\ r_0 \phi(k+1) - \phi(k+2), & k < K. \end{cases} \tag{19}$$

For Eq. (17) the initial conditions of $\theta(-1) = 0$, $\theta(0) = 1$, $\phi(K+1) = 1$, and $\phi(K+2) = 0$ are used. Since $\{\alpha, \beta, \gamma\} \in (0, 1]$, the inverse matrix $\mathbf{S}$ always exists.

The 2D target histogram $\mathbf{H}_t$ is normalized to give the target probability distribution function

$$h_{\mathrm{t}}(m', n') = h_{\mathrm{t}}(m', n') \Big/ \sum_{i=1}^{K} \sum_{j=1}^{K} h_{\mathrm{t}}(i, j). \tag{20}$$

The target CDF of $h_{\mathrm{t}}(m', n')$ is defined as

$$\mathcal{P}_{\mathrm{t}} = \left\{ P_{\mathrm{t}}(m') = \sum_{i=1}^{m'} \sum_{j=1}^{m'} h_{\mathrm{t}}(i, j) \;\middle|\; m' = 1, \ldots, K \right\}. \tag{21}$$

In order to enhance the image, the grey-levels of the input image are transformed to the output grey-levels for a given output range of $[y_d, y_u]$ using the CDFs $P_{\mathrm{x}}(m)$ and $P_{\mathrm{t}}(m')$. The input grey-level x_m is mapped to the output grey-level $y_{m'}$ by finding an index m' for a given index m according to

$$m' = \underset{i \in \{1,2,\ldots,K\}}{\operatorname{argmin}} |P_{\mathrm{x}}(m) - P_{\mathrm{t}}(i)|. \tag{22}$$

Using Eq. (22), each distinct grey-level of the input image $\mathbf{X}$ is transformed to a corresponding output grey-level to create an enhanced output image $\mathbf{Y}$. The resultant enhanced image is shown in Fig. 3(a) for $[y_d, y_u] = [0, 255]$ with the input to output grey-level data mapping shown in Fig. 3(b) and the 2D target histogram $\mathbf{H}_{\mathrm{t}}$ shown in Fig. 3(c) for $\alpha = \beta = \gamma = 1/3$. CVC increases the image brightness while keeping the high contrast between object regions.

B. Colour Image Enhancement

One approach to extend the contrast enhancement to colour images is to apply the algorithm to their luminance component (Y) only and preserve the chrominance components. Another is to multiply the chrominance values with the ratio of their input and output luminance values to preserve the hue. The former approach is employed in this paper. The *YUV* colour space [1] is selected because the conversion between *RGB* and *YUV* colour spaces is linear which considerably reduces the computational complexity for contrast enhancement in colour images. Fig. 4 shows the enhancement of the *Baboon* colour image. It shows that the contrast of the input image has been increased while the details of the input image are retained.

III. Experimental Results

A. Dataset and Quantitative Measures

We use standard test images from the datasets in [19]–[21] to evaluate and compare CVC, both qualitatively and quantitatively, with our implementations of WTHE [9], FHSABP [15], the weighted histogram approximation of HMF [16], and CEBGA

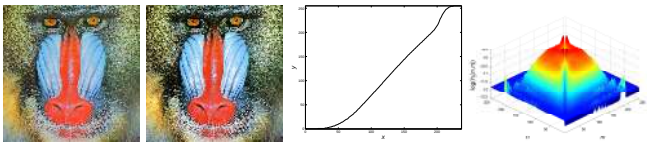

Fig. 4. Enhancing the input image *Baboon* using CVC with $\alpha = \beta = \gamma = 1/3$: (a) Input image; (b) Enhanced image; (c) Input ($\mathcal{X}$) to output ($\mathcal{Y}$) grey-level data mapping; and (d) The 2D target histogram $\mathbf{H}_{\mathrm{t}}$.

[17]. The tests of significance of the quantitative measures are performed on 500 natural images of Berkeley dataset [21]. The parameter of HMF is set by maximizing its performance for a given input image in terms of visual quality and quantitative measures. For CVC, we use $w \times w = 7 \times 7$ neighbourhood around each pixel and $\alpha = \beta = \gamma = 1/3$.

It is not easy to assess image enhancement since it is difficult to quantify an improved perception of an image. Nevertheless, in practice it is desirable to have both quantitative and subjective assessments. We use absolute mean brightness error (*AMBE*) [6], discrete entropy (*DE*) [22] and measure of enhancement (*EME*) [12], [13] as quantitative measures. For colour images, the contrast enhancement is quantified by computing these measures on their luminance channel only.

For an input image $\mathbf{X}$ and output image $\mathbf{Y}$, the absolute mean brightness error (*AMBE*) is defined as

$$AMBE\left(\mathbf{X},\mathbf{Y}\right) = \left|MB\left(\mathbf{X}\right) - MB\left(\mathbf{Y}\right)\right|, \tag{23}$$

where $MB\left(\mathbf{X}\right)$ and $MB\left(\mathbf{Y}\right)$ are the mean brightness of $\mathbf{X}$ and $\mathbf{Y}$, respectively. The lower the value of *AMBE* the better is the preservation of the original image brightness.

The discrete entropy (*DE*) of an image $\mathbf{X}$ is

$$DE\left(\mathbf{X}\right) = -\sum_{i=0}^{255} p\left(x_i\right) \log p\left(x_i\right), \tag{24}$$

where $p\left(x_i\right)$ is the probability of pixel intensity x_i which is estimated from the normalized histogram. A higher value of *DE* indicates the image has richer details.

Let the input image be divided into $k_1 k_2$ non-overlapping sub-blocks $\mathbf{X}_{i,j}$ of size $w_1 \times w_2$. *EME* is computed as

$$EME\left(\mathbf{X}\right) = \frac{1}{k_1 k_2} \sum_{i=1}^{k_1} \sum_{j=1}^{k_2} 20 \ln \frac{\max\left(\mathbf{X}_{i,j}\right)}{\min\left(\mathbf{X}_{i,j}\right)}, \tag{25}$$

where $\max\left(\mathbf{X}_{i,j}\right)$ and $\min\left(\mathbf{X}_{i,j}\right)$ are the maximum and minimum grey levels in block $\mathbf{X}_{i,j}$, respectively. A different block size (i.e., $w_1 \times w_2$) results in different *EME* value, and we use $w_1 \times w_2 = 8 \times 8$. High contrast sub-blocks give a high *EME* value, while for homogeneous sub-blocks the *EME* value should be close to zero. It is worth to note that *EME* is highly sensitive to noise. For example, if the algorithm produces an output image which introduces noise over homogeneous regions of the image, then although the output image will not look natural its corresponding *EME* value will be high. However, for a contrast enhancement algorithm it is, at least, expected that $EME\left(\mathbf{Y}\right) > EME\left(\mathbf{X}\right)$.

B. Qualitative Assessment

1) Grey-Scale Images: Some example contrast enhancement results for grey-scale images are shown in Fig. 5 and Fig. 6. The input to output grey-level mapping functions resulted from different algorithms are shown in Fig. 7(a)-(b).

For the *Tank* image [19] shown in Fig. 5(a), the mean brightness values is 127, thus although FHSABP has increased the contrast between different regions of the input image, the contrast within each region of the image is considerably reduced, and thus most of the texture of the tank is not identifiable. FHSABP maps the grey-level range of $[12, 109]$ to $[0, 30]$, and thus a

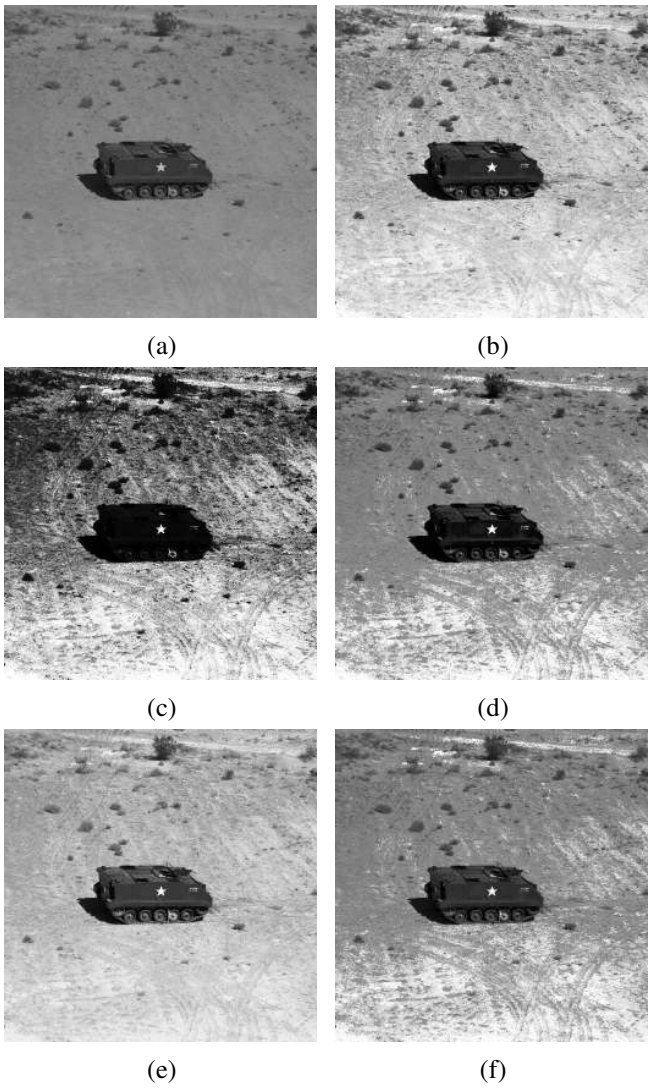

Fig. 5. Test image *Tank*. (a) Original image (*DE*=3.50, *EME*=6.56). Enhanced images generated by: (b) WTHE (*AMBE*=47.63, *DE*=3.50, *EME*=14.18); (c) FHSABP (*AMBE*=5.51, *DE*=3.39, *EME*=32.18); (d) HMF (*AMBE*=16.78, *DE*=3.45, *EME*=17.27); (e) CEBGA (*AMBE*=51.76, *DE*=2.97, *EME*=10.10); and (f) CVC (*AMBE*=22.09, *DE*=3.49, *EME*=14.42).

darkening effect on the tank region is easily noticed. WTHE and HMF provide similar high contrast images but the photometric difference between the tank and its shadow is not high enough. The similarity is confirmed by their mapping functions. CEBGA provides satisfactory contrast enhancement while retaining an overall natural look. Its performance is similar to WTHE and HMF except for lower grey-levels where it provides brighter output, and for higher grey-levels it provides darker output. CVC improves the overall contrast while preserving the image details. It is easy to identify the texture of the ground as well as the tank.

For the *Cameraman* image [19] in Fig. 6(a) the mean brightness value is 119. FHSABP maps input range of $[7, 15]$ to $[0, 33]$. Due to the low-range to higher-range mapping, it is easy to identify the details of the coat. However, there are degradation on the sky and cameraman's face. WTHE behaves similarly to FHSABP as it produces a similar shaped mapping function. The degradations on the sky and cameraman's face are not as severe as in the result by FHSABP, however the details of the coat cannot be recognized easily. HMF improves the contrast significantly with slight degradation on the sky, but it is hard to identify the details on the coat. This is mainly due to the mapping of $[7, 15]$ to $[0, 14]$. Due to the high contrast between the

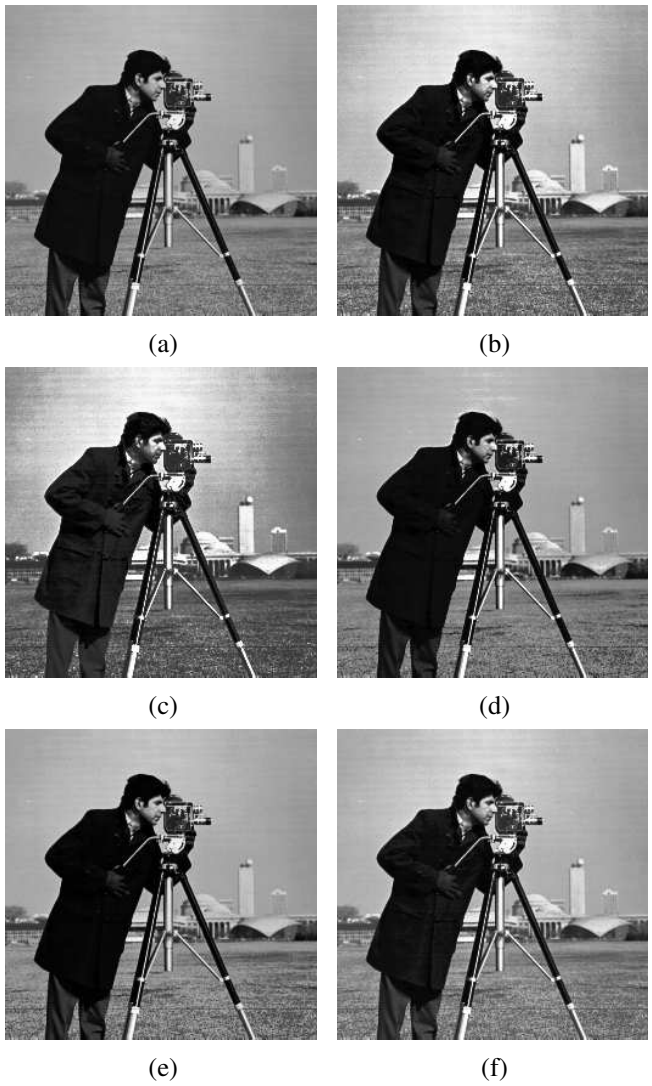

Fig. 6. Test image *Cameraman*. (a) Original image (*DE*=4.86, *EME*=16.49). Enhanced images generated by: (b) WTHE (*AMBE*=10.42, *DE*=4.80, *EME*=22.05); (c) FHSABP (*AMBE*=0.83, *DE*=4.68, *EME*=23.78); (d) HMF (*AMBE*=2.84, *DE*=4.73, *EME*=20.93); (e) CEBGA (*AMBE*=0.68, *DE*=4.47, *EME*=24.17); and (f) CVC (*AMBE*=9.47, *DE*=4.81, *EME*=18.91).

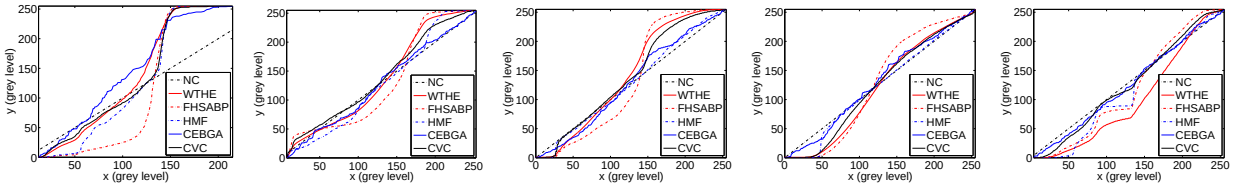

Fig. 7. Mapping functions of enhanced images where NC refers to no-change mapping: (a) Fig. 5; (b) Fig. 6; (c) Fig. 8; (d) Fig. 9; and (e) Fig. 10.

coat and the background, CEBGA only achieves a slight enhancement. This is confirmed by its mapping function being almost parallel to the no-change mapping function. CVC produces increased contrast, the details of the coat are easily identified, and the enhanced image is free of any degradation.

2) Colour Images: Some example contrast enhancement results for colour images are shown in Fig. 8 to Fig. 10. The input to output grey-level mapping functions on the luminance channel of the colour images resulted from different algorithms are shown in Fig. 7(c)-(e).

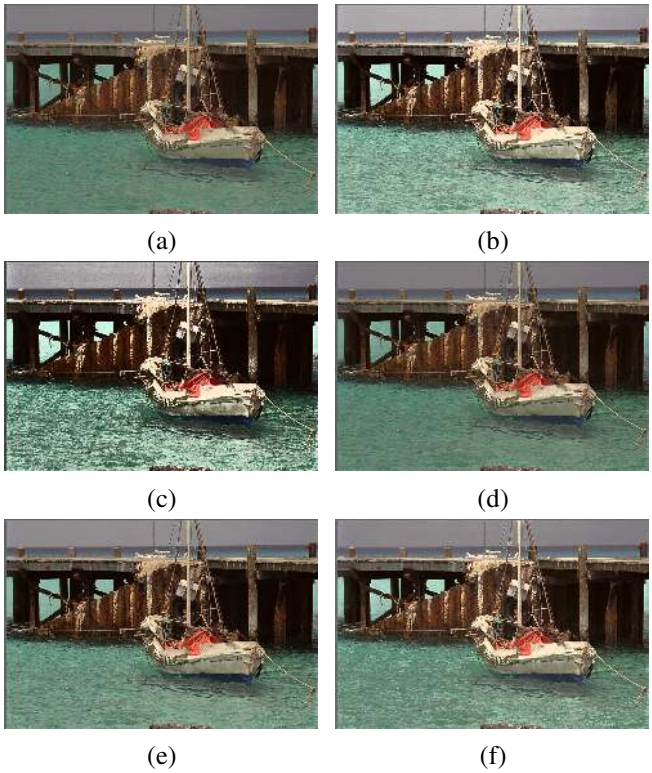

Fig. 8. Test image *Fishingboat*. (a) Original image (*DE*=4.78, *EME*=12.59). Enhanced images generated by: (b) WTHE (*AMBE*=18.64, *DE*=4.98, *EME*=17.30); (c) FHSABP (*AMBE*=1.48, *DE*=4.56, *EME*=21.45); (d) HMF (*AMBE*=1.00, *DE*=4.73, *EME*=13.72); (e) CEBGA (*AMBE*=3.39, *DE*=4.48, *EME*=15.95); and (f) CVC (*AMBE*=9.30, *DE*=4.73, *EME*=15.37).

For the *Fishingboat* image [20] in Fig. 8(a) with mean brightness value of 114, FHSABP darkens some areas of sky, sea and dock, and brightens the parts of boat and dock. There are loss of details in the darkened and brightened regions. WTHE produces a natural looking enhanced image but the dock region near the boat is darkened which makes it difficult to see the columns of the dock. Since the mapping functions of HMF and CEBGA are both similar to the no-change mapping they produce only a slight increase in contrast. CVC increases both the contrast and the average brightness to improve the overall image quality with clearer details, e.g., on the dock.

For the *Mountain* image [20] in Fig. 9(a) the mean brightness value is 128.5. WTHE and FHSABP cause the trees to be too dark for their details to be visible by mapping the input grey-level range of $[0, 50]$ to output grey-level ranges of $[0, 10]$, and $[0, 4]$, respectively. The high to low range mapping causes loss of details for regions of trees. Due to the mapping functions being almost parallel to the no-change mapping function HMF and CEBGA increase the overall contrast slightly. CVC increases both the contrast and the average brightness to improve the overall image quality. The details in the image are also clearer.

Finally, the *Cessna* image [21] in Fig. 10(a) with mean brightness value of 163 shows a Cessna plane against a bright blue sky partly covered with white clouds. The image consists of very bright and dark regions which make it challenging for a contrast enhancement algorithm. WTHE darkens the Cessna plane making it difficult for its details to be observed. FHSABP produces an enhancement better than WTHE, but a slight darkening effect can be observed on the plane. HMF produces satisfactory enhancement but over darkens the part of blue sky at the top of the enhanced image. CEBGA and CVC produce satisfactory results.

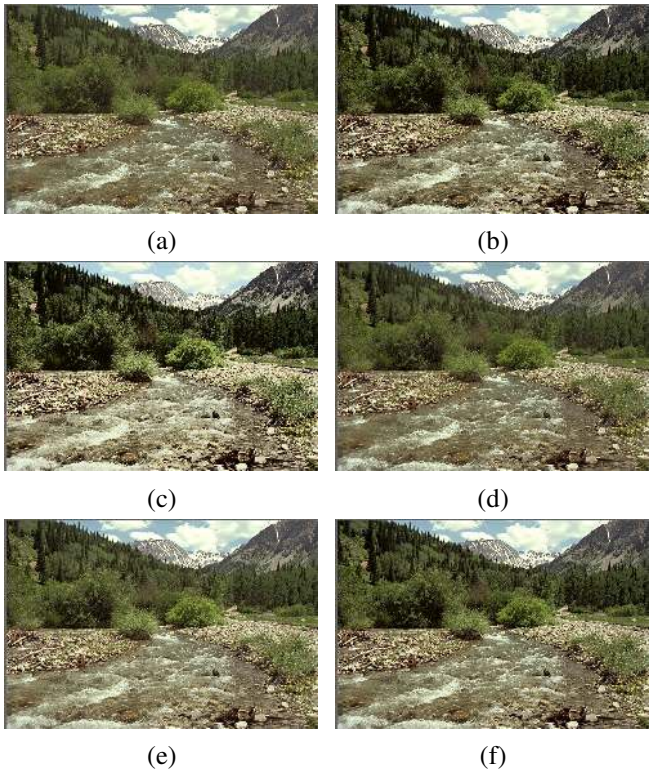

Fig. 9. Test image *Mountain*. (a) Original image (*DE*=5.15, *EME*=18.27). Enhanced images generated by: (b) WTHE (*AMBE*=7.82, *DE*=5.35, *EME*=28.37); (c) FHSABP (*AMBE*=1.40, *DE*=4.99, *EME*=31.02); (d) HMF (*AMBE*=1.01, *DE*=5.15, *EME*=20.87); (e) CEBGA (*AMBE*=5.30, *DE*=4.56, *EME*=21.09); and (f) CVC (*AMBE*=1.84, *DE*=5.11, *EME*=25.72).

TABLE I

THE p-VALUES OF HYPOTHESES EQ. (26), EQ. (27) AND EQ. (28) RESULTED FROM KS-TEST FOR DIFFERENT ALGORITHMS.

Hypothesis	WTHE	FHSABP	HMF	CEBGA	CVC
Eq. (26)	0.000000	0.988538	0.000001	0.000003	0.077420
Eq. (27)	0.000000	0.000000	0.046678	0.000000	0.403103
Eq. (28)	0.997970	0.905217	0.848223	0.253143	0.997970

C. Quantitative Assessment

In order to evaluate the performance of the five algorithms for a wide range of images, they are applied to 500 test images of Berkeley image dataset [21]. Sets of *MB*, *DE* and *EME* are computed from the original and enhanced images. The values from the original images are sorted in ascending order and the images are indexed accordingly (see Fig. 11). The sets computed on all enhanced images $\{\mathbf{Y}_i\}_{\forall i}$ resulted from an algorithm are compared with the sets computed on all original images $\{\mathbf{X}_i\}_{\forall i}$ to statistically determine if the algorithm satisfies an expected measurement criterion. Two hypotheses are proposed for each criterion: null hypothesis H_0 and alternative hypothesis H_1. The non-parametric two-sample Kolmogorov-Smirnov test (KS-test) [23] is used to reject one of the hypotheses. The KS-test tries to quantify the logical relation $(=, >, <)$ between two datasets by assigning a p-value and has the advantage of making no assumption about the distribution of the data. The p-value gives the probability of obtaining a test statistic at least as extreme as would be observed under the null hypothesis [23]. Thus the higher the p-value, the stronger the null hypothesis is. Using the p-value together with the significance level of %95, H_0 is rejected in favour of H_1 if p-value < 0.05.

In order to keep the visual correspondence between original and enhanced images in terms of brightness, the mean brightness

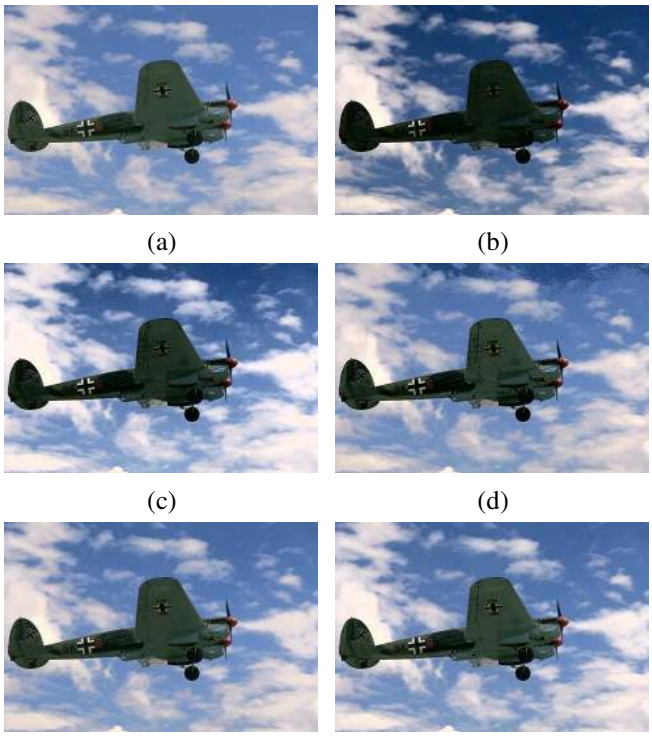

Fig. 10. Test image *Cessna*. (a) Original image (*DE*=4.97, *EME*=4.82). Enhanced images generated by: (b) WTHE (*AMBE*=29.21, *DE*=4.90, *EME*=8.78); (c) FHSABP (*AMBE*=0.31, *DE*=4.81, *EME*=8.00); (d) HMF (*AMBE*=4.31, *DE*=4.85, *EME*=7.76); (e) CEBGA (*AMBE*=0.51, *DE*=4.59, *EME*=5.44); and (f) CVC (*AMBE*=1.59, *DE*=4.92, *EME*=6.29).

values of original and enhanced images should be proportional. The *MB* values of original and enhanced images shown in the first column of Fig. 11 reveal that FHSABP, HMF, CEBGA and CVC produce enhanced images which have mean brightness values proportional to that of the original images. The closest match between mean brightness values of original and enhanced images being achieved by FHSABP and followed by CVC. In order to support the observations from Fig. 11, tests of significance are performed for each algorithm. With regard to brightness preservation, for a given test image $\mathbf{X}_i$ and its corresponding enhanced image $\mathbf{Y}_i$ resulted from one of the algorithms, one expects that $MB(\mathbf{X}_i)$ should be close to $MB(\mathbf{Y}_i)$. Thus we check whether the set of mean brightnesses of the input images $\{MB(\mathbf{X}_i)\}_{\forall i}$ and the set of mean brightnesses of the output images $\{MB(\mathbf{Y}_i)\}_{\forall i}$ are similar. The null hypothesis H_0 proposes that the algorithm produces a mean brightness which is close to the mean brightness value of the original image, while the alternative hypothesis H_1 proposes otherwise, i.e.,

$$\begin{aligned} H_0 &: \text{ the mean brightness is preserved;} \\ H_1 &: \text{ the mean brightness is not preserved.} \end{aligned} \tag{26}$$

The above hypotheses are tested for each algorithm using the KS-test and the resulting p-values are shown in Table I. According to confidence level of 95%, only FHSABP and CVC do not reject H_0 of Eq. (26), while the others reject it in favour of H_1. Thus, only FHSABP and CVC statistically produce enhanced images which have similar mean brigthness values with that of the original images.

The discrete entropy *DE* measures the information content in an image. Thus an enhancement algorithm should preserve *DE*. The *DE* values of original and enhanced images shown in the second column of Fig. 11 reveal that CVC achieves the best *DE* preservation and followed by HMF. In order to test if an algorithm achieves *DE* preservation, the sets $\{DE(\mathbf{X}_i)\}_{\forall i}$ and $\{DE(\mathbf{Y}_i)\}_{\forall i}$ resulted from original and enhanced images, respectively, are used. For each algorithm the KS-test is applied to

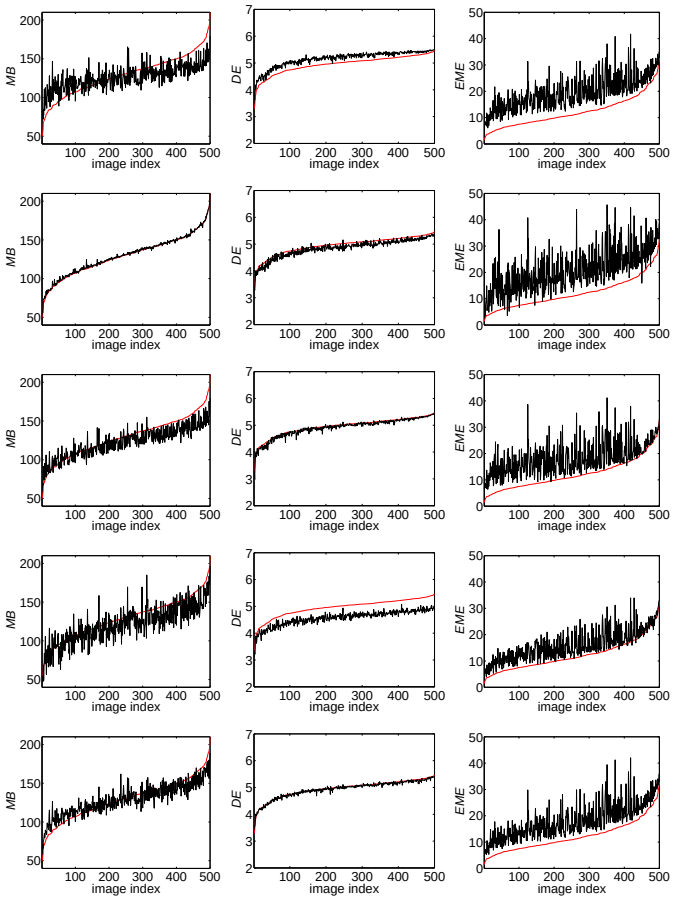

Fig. 11. Quantitative performance results on 500 colour images from Berkeley dataset [21]: the first, second, third, fourth, and fifth rows correspond respectively to WTHE, FHSABP, HMF, CEBGA and CVC. The measurements from the original images are coded in red, while those from the images enhanced using different algorithms are coded in black.

the following hypotheses:

$$\begin{aligned} H_0 &: \text{ the discrete entropy is preserved;} \\ H_1 &: \text{ the discrete entropy is not preserved.} \end{aligned} \tag{27}$$

The resulting p-values are shown in Table I. Except for CVC, all algorithms reject H_0 in favour of H_1, i.e., statistically only CVC preserves the image contents.

The *EME* values are shown in the third column of Fig. 11. Although a high *EME* does not always mean a good and natural enhancement, it is at least expected that the *EME* of an enhanced image is higher than that of its original image. For each algorithm the KS-test is applied to the following hypotheses:

$$\begin{aligned} H_0 &: \text{ the contrast is improved;} \\ H_1 &: \text{ the contrast is not improved.} \end{aligned} \tag{28}$$

The null hypothesis H_0 proposes that an enhanced image has a higher contrast than that of the original image, i.e., $\{EME(\mathbf{Y}_i) \geq EME(\mathbf{X}_i)\}_{\forall i}$. The resulting p-values are shown in Table I. According to 95% confidence level, all algorithms do not reject H_0. Thus, statistically all algorithms produce higher contrast enhanced images. The p-values also indicate that WTHE and CVC equally provide the best performances while CEBGA the worst.

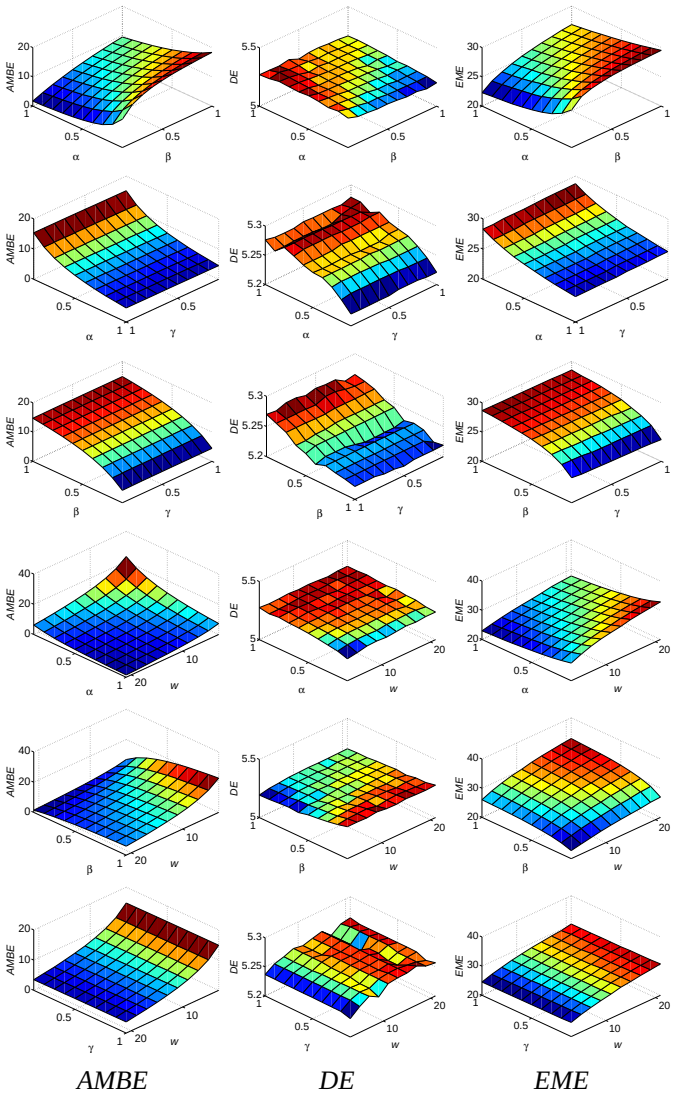

Fig. 12. Quantitative measurement results as *AMBE*, *DE*, and *EME* of the enhanced *Baboon* images using CVC for different values of w, α, β and γ. (row 1) Varying α and β with $w = 7$, $\gamma = 1/3$. (row 2) Varying α and γ with $w = 7$, $\beta = 1/3$. (row 3) Varying β and γ with $w = 7$, $\alpha = 1/3$. (row 4) Varying α and w with $\beta = 1/3$, $\gamma = 1/3$. (row 5) Varying β and w with $\alpha = 1/3$, $\gamma = 1/3$. (row 6) Varying γ and w with $\alpha = 1/3$, $\beta = 1/3$.

D. The Effect of Different Parameter Settings

The $w \times w$ spatial support of the neighbourhood around each pixel, α, β, and γ are the tuning parameters of CVC. The results presented in Section III-B and Section III-C are for the default setting of $w = 7$, $\alpha = \beta = \gamma = 1/3$. Although the default setting provides satisfactory results, further improvement can be achieved by varying the parameters. To demonstrate the effects of varying the parameters, the *Baboon* image shown in Fig. 4(a) is enhanced for different values of w, α, β and γ. In order to see the effects of the parameters on the performance of the enhancement using the quantitative measures, two parameters are set to their default values while the other two parameters are varied.

The resulting quantitative measures are shown in Fig. 12. An increase in the value of α results in lower *AMBE*, higher *DE* and lower *EME*, and vice versa. The higher the value of α, the more contribution from the 2D input histogram $\mathbf{H}_{\mathrm{x}}$ which results in an enhanced image which is similar to the input image. This similarity lowers the value of *AMBE*, preserves the overall content which results in higher *DE*, however it also lowers the *EME* since there will be not much difference between the input and output images. The increase in the value of β increases the contribution of the 2D uniformly distributed histogram

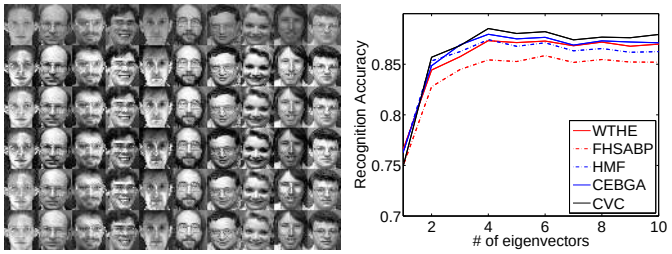

(a) (b)

Fig. 13. (a) Contrast enhanced images resulted from applying different algorithms on sample images from ORL face database [24]: the first, second, third, fourth, fifth, and sixth rows correspond respectively to the original images and images enhanced by WTHE, FHSABP, HMF, CEBGA and CVC. (b) Face recognition on ORL face database [24] using 2DPCA [25] on images enhanced by different algorithms.

$\mathbf{H}_{\mathrm{u}}$, thus the resultant image will have a higher contrast. This will result in high value of *EME*, however due to decreased similarity between input and output images, the value of *AMBE* increases and the value of *DE* decreases. The change in γ does not change the values of *AMBE*, *DE* and *EME* significantly, since γ contributes to the smoothness of the 2D target histogram. The plots for *AMBE*, *DE*, and *EME* suggest that CVC achieves better enhancement with a larger $w \times w$ local support. This is as expected since a larger value of w results in a better representation of contextual information.

E. The Effect of Contrast Enhancement on Object Recognition

Contrast enhancement is often applied as a pre-processing for object recognition. However, the performance of a contrast enhancement algorithm affects the object recognition process. To demonstrate the effects, face is selected as an object, and face recognition is performed on images of the ORL face database [24] enhanced by different methods. The face recognition task is achieved as follows. For each subject in the database, a set of training images is stored. The training database is represented by a set of eigenvectors which are computed using 2DPCA. Each training image is projected onto the eigenvectors, and a set of projection vectors is stored for each subject. The query face is identified according to the minimum Euclidean distance between its projection vectors and the projection vectors of the subjects in database. The number of eigenvectors determines the face recognition rate.

The ORL face database [24] contains images of 40 subjects, each providing 10 different images. All images are grey-scale and normalized to a resolution of 112×92 pixels. An enhanced sample image of each of 10 subjects using different algorithms are shown in Fig. 13(a). For each subject in the database, five images are used for training and the remaining five images for query (testing) images. Thus, the total number of training samples and testing samples are both 200. The recognition results in Fig. 13(b) show that the face recognition is consistently best on images enhanced by CVC. This indicates that not only CVC improves the contrast, it also preserves the overall content of the image.

F. Computational Complexity

The computational complexities of the different algorithms except CEBGA are analysed for an input image of size $H \times W$ pixels with K distinct grey levels. The analysis is performed only for grey-scale images as it is assumed that the same procedure of processing only the intensity channel of colour image is followed by the all algorithms when a colour image is processed. Since CEBGA employs GA to perform evolutionary contrast enhancement, it is difficult to perform such an analysis. However, it is empirically observed that CEBGA demands the highest computational time.

TABLE II

COMPUTATIONAL TIME COMPLEXITY ANALYSIS OF CONTRAST ENHANCEMENT ALGORITHMS FOR AN INPUT IMAGE OF SIZE $H \times W$ PIXELS WITH K DISTINCT GREY LEVELS. KEY TO PROCESS LABELS: A - COMPUTES 1D/2D HISTOGRAM; B - UPDATES HISTOGRAM; C - COMPUTES MAPPING FUNCTION; AND D - GENERATES OUTPUT IMAGE.

	Algorithm			
Process	WTHE	FHSABP	HMF	CVC
A	$\mathcal{O}(HW)$	$\mathcal{O}(HW)$	$\mathcal{O}(HW)$	$\mathcal{O}(HW(w^2-1))$
B	$\mathcal{O}(K)$	–	$\mathcal{O}(K)$	$\mathcal{O}(K^2)$
C	$\mathcal{O}(K)$	$\mathcal{O}(HW+K)$	$\mathcal{O}(K)$	$\mathcal{O}(K^3+K^2)$
D	$\mathcal{O}(HW)$	$\mathcal{O}(HW)$	$\mathcal{O}(HW)$	$\mathcal{O}(HW)$
Total	$\mathcal{O}(2HW+2K)$	$\mathcal{O}(3HW+K)$	$\mathcal{O}(2HW+2K)$	$\mathcal{O}(HWw^2+K^3+2K^2)$

The computational time complexity analysis of different algorithms are summarised in Table II. The computational time complexity of CVC is higher than WTHE, FHSABP and HMF, but lower than CEBGA. Although CVC demands higher computation time, it can be easily implemented on a moderate processor with high computational efficiency.

IV. CONCLUSIONS

In this paper, we proposed an enhancement algorithm, CVC, which employs contextual data modelling using 2D histogram of an input image to perform non-linear data mapping for generating visually pleasing enhancement on different types of images. CVC can be applied to both grey-level and colour images using the default setting of the tuning parameters. Performance comparisons with state-of-the-art enhancement algorithms show that CVC achieves satisfactory image equalization even under diverse illumination conditions.

By achieving high discrete entropy preservation between the input and output images, CVC preserves the overall content of an input image while providing sufficient contrast enhancement. This is mainly because CVC employs contextual information between pixels and their neighbours. Since the conservation of the entropy is utmost important for several applications which require enhancement as a preprocessing, such as face recognition, CVC can be applied for such a requirement. It is also shown that the recognition results on images enhanced by CVC is higher than those enhanced by the other enhancement algorithms considered in this work.

Using the tests of significance on 500 natural images from Berkeley dataset, it is shown that CVC achieves brightness preservation, discrete entropy preservation, and contrast improvement under 95% confidence level.

APPENDIX

The following properties of matrix trace are used in the derivation of Eq. (15) where matrices and scalars are shown in bold and italic fonts, respectively: $\mathrm{tr}\,(\mathbf{A}) = \mathrm{tr}\,(\mathbf{A}^{\mathrm{T}})$, $\mathrm{tr}\,(k\mathbf{B}) = k\mathrm{tr}\,(\mathbf{B})$, $\mathrm{tr}\,(\mathbf{AB}) = \mathrm{tr}\,(\mathbf{BA})$, $\mathrm{tr}\,(\mathbf{A}+\mathbf{B}) = \mathrm{tr}\,(\mathbf{A}) + \mathrm{tr}\,(\mathbf{B})$, $\boldsymbol{\nabla}_{\mathbf{A}}\mathrm{tr}\,(\mathbf{AB}) = \mathbf{B}^{\mathrm{T}}$, and $\boldsymbol{\nabla}_{\mathbf{A}}\mathrm{tr}\,(\mathbf{ABA}^{\mathrm{T}}\mathbf{C}) = \mathbf{CAB} + \mathbf{C}^{\mathrm{T}}\mathbf{AB}^{\mathrm{T}}$.

$$\begin{aligned}\nabla_{\mathbf{H}} f(\mathbf{H}) &= \boldsymbol{\nabla}_{\mathbf{H}} \Big[\boldsymbol{\alpha}\ \mathrm{tr}\left((\mathbf{H}-\mathbf{H}_{\mathrm{x}})(\mathbf{H}-\mathbf{H}_{\mathrm{x}})^{\mathrm{T}}\right)+ \\ &\quad \beta\ \mathrm{tr}\left((\mathbf{H}-\mathbf{H}_{\mathrm{u}})(\mathbf{H}-\mathbf{H}_{\mathrm{u}})^{\mathrm{T}}\right)+ \\ &\quad \gamma\ \mathrm{tr}\left(\mathbf{HD}(\mathbf{HD})^{\mathrm{T}}\right)\Big] \\ &= \boldsymbol{\alpha}\boldsymbol{\nabla}_{\mathbf{H}}\ \mathrm{tr}\left((\mathbf{H}-\mathbf{H}_{\mathrm{x}})(\mathbf{H}-\mathbf{H}_{\mathrm{x}})^{\mathrm{T}}\right)+ \\ &\quad \boldsymbol{\beta}\boldsymbol{\nabla}_{\mathbf{H}}\ \mathrm{tr}\left((\mathbf{H}-\mathbf{H}_{\mathrm{u}})(\mathbf{H}-\mathbf{H}_{\mathrm{u}})^{\mathrm{T}}\right)+ \\ &\quad \boldsymbol{\gamma}\boldsymbol{\nabla}_{\mathbf{H}}\ \mathrm{tr}\left(\mathbf{HD}(\mathbf{HD})^{\mathrm{T}}\right).\end{aligned}$$

The term $\mathrm{tr}\left((\mathbf{H}-\mathbf{H}_{\mathrm{x}})(\mathbf{H}-\mathbf{H}_{\mathrm{x}})^{\mathrm{T}}\right)$ is expanded as

$$\begin{aligned}&\mathrm{tr}\left((\mathbf{H}-\mathbf{H}_{\mathrm{x}})(\mathbf{H}-\mathbf{H}_{\mathrm{x}})^{\mathrm{T}}\right) \\ &= \mathrm{tr}\left(\mathbf{HH}^{\mathrm{T}}-\mathbf{HH}_{\mathrm{x}}^{\mathrm{T}}-\mathbf{H}_{\mathrm{x}}\mathbf{H}^{\mathrm{T}}+\mathbf{H}_{\mathrm{x}}\mathbf{H}_{\mathrm{x}}^{\mathrm{T}}\right) \\ &= \mathrm{tr}\left(\mathbf{HH}^{\mathrm{T}}\right)-\mathrm{tr}\left(\mathbf{HH}_{\mathrm{x}}^{\mathrm{T}}\right)-\mathrm{tr}\left(\mathbf{H}_{\mathrm{x}}\mathbf{H}^{\mathrm{T}}\right)+\mathrm{tr}\left(\mathbf{H}_{\mathrm{x}}\mathbf{H}_{\mathrm{x}}^{\mathrm{T}}\right) \\ &= \mathrm{tr}\left(\mathbf{HH}^{\mathrm{T}}\right)-2\mathrm{tr}\left(\mathbf{HH}_{\mathrm{x}}^{\mathrm{T}}\right)+\mathrm{tr}\left(\mathbf{H}_{\mathrm{x}}\mathbf{H}_{\mathrm{x}}^{\mathrm{T}}\right),\end{aligned}$$

where $\mathrm{tr}\left(\mathbf{HH}_{\mathrm{x}}^{\mathrm{T}}\right)=\mathrm{tr}\left(\mathbf{H}_{\mathrm{x}}\mathbf{H}^{\mathrm{T}}\right)$. Hence,

$$\begin{aligned}&\boldsymbol{\nabla}_{\mathbf{H}}\mathrm{tr}\left((\mathbf{H}-\mathbf{H}_{\mathrm{x}})(\mathbf{H}-\mathbf{H}_{\mathrm{x}})^{\mathrm{T}}\right) \\ &= \boldsymbol{\nabla}_{\mathbf{H}}\left[\mathrm{tr}\left(\mathbf{HH}^{\mathrm{T}}\right)-\mathbf{2}\mathrm{tr}\left(\mathbf{HH}_{\mathrm{x}}^{\mathrm{T}}\right)+\mathrm{tr}\left(\mathbf{H}_{\mathrm{x}}\mathbf{H}_{\mathrm{x}}^{\mathrm{T}}\right)\right] \\ &= \boldsymbol{\nabla}_{\mathbf{H}}\mathrm{tr}\left(\mathbf{HH}^{\mathrm{T}}\right)-\mathbf{2}\boldsymbol{\nabla}_{\mathbf{H}}\mathrm{tr}\left(\mathbf{HH}_{\mathrm{x}}^{\mathrm{T}}\right)+\boldsymbol{\nabla}_{\mathbf{H}}\mathrm{tr}\left(\mathbf{H}_{\mathrm{x}}\mathbf{H}_{\mathrm{x}}^{\mathrm{T}}\right) \\ &= 2\mathbf{H}-2\mathbf{H}_{\mathrm{x}}+\mathbf{0}.\end{aligned}$$

Thus $\boldsymbol{\nabla}_{\mathbf{H}}\mathrm{tr}\left((\mathbf{H}-\mathbf{H}_{\mathrm{u}})(\mathbf{H}-\mathbf{H}_{\mathrm{u}})^{\mathrm{T}}\right)=\mathbf{2H}-\mathbf{2H}_{\mathrm{u}}+\mathbf{0}$. Similarly, one can expand $\boldsymbol{\nabla}_{\mathbf{H}}\ \mathrm{tr}\left(\mathbf{HD}(\mathbf{HD})^{\mathrm{T}}\right)$ as

$$\begin{aligned}\boldsymbol{\nabla}_{\mathbf{H}}\ \mathrm{tr}\left(\mathbf{HD}(\mathbf{HD})^{\mathrm{T}}\right) &= \boldsymbol{\nabla}_{\mathbf{H}}\ \mathrm{tr}\left(\mathbf{HDD}^{\mathrm{T}}\mathbf{H}^{\mathrm{T}}\right) \\ &= \boldsymbol{\nabla}_{\mathbf{H}}\ \mathrm{tr}\left(\mathbf{HDD}^{\mathrm{T}}\mathbf{H}^{\mathrm{T}}\mathbf{I}\right) \\ &= \mathbf{IHDD}^{\mathrm{T}}+\mathbf{I}^{\mathrm{T}}\mathbf{H}\left(\mathbf{DD}^{\mathrm{T}}\right)^{\mathrm{T}} \\ &= \mathbf{HDD}^{\mathrm{T}}+\mathbf{HDD}^{\mathrm{T}}=2\mathbf{HDD}^{\mathrm{T}}.\end{aligned}$$

Hence,

$$\begin{aligned}\nabla_{\mathbf{H}} f(\mathbf{H}) &= 2\alpha(\mathbf{H}-\mathbf{H}_{\mathrm{x}})+2\beta(\mathbf{H}-\mathbf{H}_{\mathrm{u}})+2\gamma\mathbf{HDD}^{\mathrm{T}} \\ &= 2\left[\left((\alpha+\beta)\mathbf{I}+\gamma\mathbf{DD}^{\mathrm{T}}\right)\mathbf{H}-\alpha\mathbf{H}_{\mathrm{x}}-\beta\mathbf{H}_{\mathrm{u}}\right],\end{aligned}$$

where $\mathbf{I}$ is identity matrix. The solution is obtained by setting $\nabla_{\mathbf{H}} f(\mathbf{H}) = \mathbf{0}$ which yields to $\mathbf{H} = \left((\alpha+\beta)\mathbf{I}+\gamma\mathbf{DD}^{\mathrm{T}}\right)^{-1}(\alpha\mathbf{H}_{\mathrm{x}}+\beta\mathbf{H}_{\mathrm{u}})$.

REFERENCES

[1] R. C. Gonzalez and R. E. Woods, *Digital Image Processing (3rd Edition)*. Upper Saddle River, NJ, USA: Prentice-Hall, Inc., 2006.

[2] R. Dale-Jones and T. Tjahjadi, "A study and modification of the local histogram equalization algorithm," *Pattern Recognit.*, vol. 26, no. 9, pp. 1373–1381, September 1993.

[3] T. K. Kim, J. K. Paik, and B. S. Kang, "Contrast enhancement system using spatially adaptive histogram equalization with temporal filtering," *IEEE Trans. Consumer Electron.*, vol. 44, no. 1, pp. 82–87, Feb 1998.

[4] Y.-T. Kim, "Contrast enhancement using brightness preserving bi-histogram equalization," *IEEE Trans. Consumer Electron.*, vol. 43, no. 1, pp. 1–8, Feb 1997.

[5] Y. Wang, Q. Chen, and B. Zhang, "Image enhancement based on equal area dualistic sub-image histogram equalization method," *IEEE Trans. Consumer Electron.*, vol. 45, no. 1, pp. 68–75, Feb 1999.

[6] S.-D. Chen and A. Ramli, "Minimum mean brightness error bi-histogram equalization in contrast enhancement," *IEEE Trans. Consumer Electron.*, vol. 49, no. 4, pp. 1310–1319, Nov 2003.

[7] ——, "Contrast enhancement using recursive mean-separate histogram equalization for scalable brightness preservation," *IEEE Trans. Consumer Electron.*, vol. 49, no. 4, pp. 1301–1309, Nov 2003.

[8] M. Abdullah-Al-Wadud, M. Kabir, M. Dewan, and O. Chae, "A Dynamic Histogram Equalization for Image Contrast Enhancement," *IEEE Trans. Consumer Electron.*, vol. 53, no. 2, pp. 593–600, May 2007.

[9] Q. Wang and R. K. Ward, "Fast image/video contrast enhancement based on weighted thresholded histogram equalization," *IEEE Trans. Consumer Electron.*, vol. 53, no. 2, pp. 757–764, May 2007.

[10] C.-C. Sun, S.-J. Ruan, M.-C. Shie, and T.-W. Pai, "Dynamic contrast enhancement based on histogram specification," *IEEE Trans. Consumer Electron.*, vol. 51, no. 4, pp. 1300–1305, Nov 2005.

[11] D. Jobson, Z. Rahman, and G. Woodell, "A multiscale retinex for bridging the gap between color images and the human observation of scenes," *IEEE Trans. Image Process.*, vol. 6, no. 7, pp. 965–976, Jul 1997.

[12] S. Agaian, B. Silver, and K. Panetta, "Transform coefficient histogram-based image enhancement algorithms using contrast entropy," *IEEE Trans. Image Process.*, vol. 16, no. 3, pp. 741–758, Mar 2007.

[13] K. Panetta, E. Wharton, and S. Agaian, "Human visual system-based image enhancement and logarithmic contrast measure," *IEEE Trans. Syst. Man Cybern. B, Cybern.*, vol. 38, no. 1, pp. 174–188, Feb 2008.

[14] J. Mukherjee and S. Mitra, "Enhancement of color images by scaling the dct coefficients," *IEEE Trans. Image Process.*, vol. 17, no. 10, pp. 1783–1794, Oct 2008.

[15] C. Wang, J. Peng, and Z. Ye, "Flattest histogram specification with accurate brightness preservation," *IET Image Process.*, vol. 2, no. 5, pp. 249–262, Oct 2008.

[16] T. Arici, S. Dikbas, and Y. Altunbasak, "A Histogram Modification Framework and Its Application for Image Contrast Enhancement," *IEEE Trans. Image Process.*, vol. 18, no. 9, pp. 1921–1935, Sep 2009.

[17] S. Hashemi, S. Kiani, N. Noroozi, and M. E. Moghaddam, "An image contrast enhancement method based on genetic algorithm," *Pattern Recognit. Lett.*, vol. 31, no. 13, pp. 1816–1824, 2010.

[18] R. A. Usmani, "Inversion of a tridiagonal jacobi matrix," *Linear Algebra and its Applications*, vol. 212-213, pp. 413–414, 1994.

[19] Retrieved on August 2010 from the World Wide Web: http://sipi.usc.edu/database/.

[20] Retrieved on August 2010 from the World Wide Web: http://r0k.us/graphics/kodak/.

[21] P. Arbelaez, M. Maire, C. Fowlkes, and J. Malik, "Contour detection and hierarchical image segmentation," *IEEE Trans. Pattern Anal. Mach. Intell.*, InPress.

[22] C. E. Shannon, "A mathematical theory of communication," *Bell Syst. Tech. J.*, vol. 27, 1948.

[23] D. J. Sheskin, *Handbook of Parametric and Nonparametric Statistical Procedures*, 4th ed. Chapman & Hall/CRC, 2007.

[24] Retrieved on November 2010 from the World Wide Web: http://www.cl.cam.ac.uk/research/dtg/attarchive/facedatabase.html.

[25] J. Yang, D. Zhang, A. Frangi, and J. yu Yang, "Two-dimensional pca: a new approach to appearance-based face representation and recognition," *IEEE Trans. Pattern Anal. Mach. Intell.*, vol. 26, no. 1, pp. 131–137, Jan 2004.

Turgay Celik received the Ph.D. degree in engineering from the University of Warwick, U.K., in 2011. He has produced extensive publications in various international journals and conferences. He has been acting as a reviewer for various international journals and conferences. His research interests are in the areas of biophysics, digital signal, image and video processing, pattern recognition and artificial intelligence, unusual event detection, remote sensing, and global optimization techniques.

Tardi Tjahjadi (SM'02) received the B.Sc. (Hons.) degree in mechanical engineering from University College London, U.K., in 1980, M.Sc. degree in management sciences (operational management) and Ph.D. in total technology from the University of Manchester Institute of Science and Technology, U.K., in 1981 and 1984, respectively. He joined the School of Engineering at the University of Warwick and the U.K. Daresbury Synchrotron Radiation Source Laboratory as a joint teaching fellow in 1984. He was appointed a lecturer in computer systems engineering at the same university in 1986, and has been an associate professor since 2000. His research interests include multiresolution image processing, image sequence processing and 3D computer vision.